

Maternal embryonic leucine zipper kinase transcript abundance correlates with malignancy grade in human astrocytomas

Suely K.N. Marie^{1*}, Oswaldo K. Okamoto², Miyuki Uno¹, Ana Paula G. Hasegawa¹, Sueli M. Oba-Shinjo¹, Tzeela Cohen³, Anamaria A. Camargo⁴, Ana Kosoy³, Carlos G. Carlotti Jr.⁵, Silvia Toledo⁶, Carlos A. Moreira-Filho⁷, Marco A. Zago⁸, Andrew J. Simpson³ and Otavia L. Caballero³

¹Department of Neurology, School of Medicine, University of São Paulo, São Paulo, Brazil

²Department of Neurology and Neurosurgery, Federal University of São Paulo, São Paulo, Brazil

³Ludwig Institute for Cancer Research, New York Branch at Memorial Sloan-Kettering Cancer Center, New York, NY

⁴Ludwig Institute for Cancer Research, São Paulo Branch at Hospital Alemão Oswaldo Cruz, São Paulo, Brazil

⁵Division of Neurosurgery, Department of Surgery, School of Medicine of Ribeirão Preto, University of São Paulo, Ribeirão Preto, Brazil

⁶Department of Pediatrics, Pediatric Oncology Institute, Federal University of São Paulo, São Paulo, Brazil

⁷Albert Einstein Research and Education Institute, São Paulo, Brazil

⁸Department of Clinical Medicine, School of Medicine of Ribeirão Preto, University of São Paulo, Ribeirão Preto, Brazil

We have performed cDNA microarray analyses to identify gene expression differences between highly invasive glioblastoma multiforme (GBM) and typically benign pilocytic astrocytomas (PA). Despite the significant clinical and pathological differences between the 2 tumor types, only 63 genes were found to exhibit 2-fold or greater overexpression in GBM as compared to PA. Forty percent of these genes are related to the regulation of the cell cycle and mitosis. QT-PCR validation of 6 overexpressed genes: *MELK*, *AUKB*, *ASPM*, *PRC1*, *IL13RA2* and *KIAA0101* confirmed at least a 5-fold increase in the average expression levels in GBM. Maternal embryonic leucine zipper kinase (*MELK*) exhibited the most statistically significant difference. A more detailed investigation of *MELK* expression was undertaken to study its oncogenic relevance. In the examination of more than 100 tumors of the central nervous system, we found progressively higher expression of *MELK* with astrocytoma grade and a noteworthy uniformity of high level expression in GBM. Similar level of overexpression was also observed in medulloblastoma. We found neither gene promoter hypomethylation nor amplification to be a factor in *MELK* expression, but were able to demonstrate that *MELK* knockdown in malignant astrocytoma cell lines caused a reduction in proliferation and anchorage-independent growth in *in vitro* assays. Our results indicate that GBM and PA differ by the expression of surprisingly few genes. Among them, *MELK* correlated with malignancy grade in astrocytomas and represents a therapeutic target for the management of the most frequent brain tumors in adult and children.

© 2007 Wiley-Liss, Inc.

Key words: glioblastoma; pilocytic astrocytoma; microarray; *MELK*; molecular target

Astrocytomas are gliomas of astrocytic origin and constitute the most common type of primary brain tumor. They are classified, according to the World Health Organization (WHO), into pilocytic astrocytomas (PA) (Grade I), low-grade astrocytomas (Grade II), anaplastic astrocytomas (Grade III) and glioblastoma multiforme (GBM) (Grade IV).^{1,2} PA, the most common glioma in children and young adults, has a good prognosis because of being more circumscribed and thus curable by total surgical resection. In contrast, astrocytomas Grade II to Grade IV are highly infiltrating and are hence named diffuse astrocytomas. These infiltrative tumors are generally not curable by resection. Despite efforts to develop novel therapies, the median survival rate of patients with GBM rarely exceeds 12 months,³ reflecting the resistance of these tumors not only to surgical approaches but also to chemotherapy and radiation therapy. Although multiple genetic alterations including chromosomal abnormalities, oncogene activation and tumor suppressor gene inactivation⁴ have already been identified in astrocytomas, the dismal prospects for patients with this disease render the identification of additional therapeutic targets as an important objective.

Gene expression patterns provide insight into the nature of the molecular alterations that lead to the establishment and progression of tumors. Genome-wide technologies such as cDNA microarrays, large-scale EST sequencing,⁵ serial analysis of gene expression⁶ (SAGE) and massive parallel signature sequencing^{7,8} (MPSS) have become powerful tools for investigating the molecular biology of malignancy, and the comparison of different grades of tumors by microarray is a well-established starting point for selecting genes of interest. In this study, we used oligonucleotide microarrays to compare the expression pattern of 10,000 genes in Grade IV (GBM) and Grade I (PA) astrocytic tumors to identify genes associated with invasion and proliferation. Among the most highly overexpressed genes in GBM was *MELK* (maternal embryonic leucine zipper kinase), which has been reported to be upregulated in several cancer types relative to normal tissues and which regulates multipotent neural progenitors.^{9,10} To investigate the potential oncogenic role of *MELK* in astrocytomas, we studied mechanisms of *MELK* overexpression by gene amplification, promoter methylation analysis, and the biological consequences of *MELK* downregulation on tumor cell proliferation, anchorage independent growth, motility and apoptosis. This data suggest that *MELK* expression increases according to the grade of malignancy in astrocytomas, and represents a potential therapeutic target.

Material and methods

Tissue samples

Tumor specimens were obtained from patients with CNS tumors treated by the Neurosurgery Group of the Department of Neurology at Hospital das Clínicas, School of Medicine, University of São Paulo, São Paulo, Brazil, between 2000 and 2005. The tissues were categorized according to the WHO grading system^{1,2} by neuropathologists from the Division of Pathological Anatomy of the same institution. Informed consent was obtained from each patient. Fresh surgical samples of different grades and nonneoplastic tissues of the CNS (temporal lobectomy from epilepsy surgeries) were macrodissected and immediately snap-frozen in liquid nitrogen upon surgical removal. All tumor tissues were microdissected before RNA extraction as described previously.¹¹ None

Grant sponsors: FAPESP, Ludwig Institute for Cancer Research (New York).

*Correspondence to: Department of Neurology, School of Medicine, University of São Paulo, Av. Dr Arnaldo 455, Cerqueira César, Room 4110, 01246-903 São Paulo, SP, Brazil. Fax: +55-113-061-4036. E-mail: sknmarie@usp.br

Received 2 April 2007; Accepted after revision 21 August 2007

DOI 10.1002/ijc.23189

Published online 24 October 2007 in Wiley InterScience (www.interscience.wiley.com).

of the patients received any other treatment than per oral dexamethazone before surgery, when the samples analyzed were collected.

Cell lines, cell suspensions, culture and reagents

Human malignant astrocytomas cell lines T98G and U87MG, obtained from the American Type Culture Collection (Manassas, VA), were cultivated in Dulbecco's modified Eagle's medium (DMEM), supplemented with 10% fetal calf serum (FCS), in a humidified incubator at 37°C and controlled CO₂ atmosphere.

Analysis of gene expression using microarrays

Nine primary astrocytomas (3 samples of PA, mean age of 19 years; and 6 samples of GBM, mean age of 56 years and mean survival time of 7.6 months), and 2 pools of 3 nonneoplastic brain tissues (mean age of 31 and 47 years) were used for microarray analyses.

Analyses were carried out with oligonucleotide microarrays representing 10,000 human genes (CodeLink Bioarrays-Human Uniset I; GE Healthcare, Piscataway, NJ), following the manufacturer's protocol. The fluorescence was measured using an Axon GenePix 4000B Scanner (Axon Instruments, Sunnyvale, CA), and normalized with the CodeLink Software v.2.3 (GE Healthcare). Independent hybridizations for each tumor sample were carried out in duplicate. Raw data and normalized hybridization data are available according to MIAME guidelines at the GEO database, under the accession number GSE7330.

Individual PA and GBM gene expression profiles were compared with each other, and with nonneoplastic brain tissue: PA with the pool of nonneoplastic brain tissue from epilepsy patients with mean age of 31 years, and GBM with the pool of mean age of 47 years. Differentially expressed genes were identified by calculating the ratio of the mean normalized fluorescence values obtained from each duplicate GBM or PA sample and nonneoplastic brain tissue pools, and subsequently between duplicate GBM and PA samples. Results were expressed as fold variation, and genes displaying greater than 2-fold changes in transcript abundance and $p < 0.01$ were selected.

Differentially expressed genes in astrocytomas were classified according to an ontology term enrichment analysis,¹² as defined by the Gene Ontology Consortium, to identify functional classes. In such analysis, the statistical association between being differentially expressed and belonging to a given category was accessed by the Fisher's exact test.

Total RNA extraction and cDNA synthesis

Total RNA was extracted from tissues or cell lines using Trizol (Invitrogen, Carlsbad, CA) or RNeasy Mini Kit (Qiagen, Hilden, Germany). Synthesis of cDNA was performed by reverse transcription, using oligo(dT) and random hexamers, and SuperScript III (Invitrogen), according to the manufacturer's recommendations.

DNA extraction

Frozen tissue DNA was extracted with a standard phenol/chloroform methodology or with Trizol (Invitrogen), following the manufacturer's instructions.

Quantitative real time RT-PCR

The relative expression levels of the genes *AURKB* (aurora kinase B), *ASPM* (abnormal spindle-like microcephaly associated), *PRC1* (protein regulator of cytokinesis 1), *IL13RA2* (interleukin 13 receptor α2), *KIAA0101* and *MELK* (maternal embryonic leucine zipper Kinase) were analyzed by QT-PCR to validate microarray data. To this end we used 7 nonneoplastic brain tissues and 18 astrocytic tumor samples (13 GBM and 5 PA). For a more detailed analysis of relative *MELK* and *PLP2* expression, we used an independent series of 10 nonneoplastic brain tissues (median age 37 years) and 93 astrocytic tumor samples: 12 PA (median

age 22 years), 13 low-grade astrocytomas (median age 37 years), 15 anaplastic astrocytomas (median age 31 years) and 53 GBM (median age 52 years). The GBM cases included in this study were primary GBM, based on the clinical history with mean interval time between the onset of symptoms and the surgical procedure of 4.3 months, low incidence (4%) of p53 mutation and high detection of *EGFR* overexpression (44%), mostly because of gene amplification.

Histologically, none of the included GBM samples presented sarcomatous or oligo component. We also examined 26 medulloblastomas (median age 18 years). All QT-PCR assays were carried out in duplicate using the Sybr-Green I approach. Normalization of quantitative data was based on the housekeeping gene, hypoxanthine guanine phosphoribosyltransferase (*HPRT*). Primer sequences were as follows (5'-3'): *AURKB* F: CTGCCATGG GAAGAAGGTGATTCA, *AURKB* R: GATGCGCGATAGGT CTCGTTG, *ASPM* F: TGTGGAGTGCCTTG, *ASPM* R: TGCCGAATCTGAGTTCT, *PRC1* F: CCTGCCCTACTGC CAAAGA, *PRC1* R: CAGAACTGAACACAATTAAACAAAG CT, *IL13RA2* F: TTGCGTAAGCCAAACACCTA, *IL13RA2* R: TGAACATTTGCCATGACTG, *KIAA0101* F: GTTTGAA CATGGTGCAGACTAA, *KIAA0101* R: GGCAGAGGTGGAA GAACCAA, *MELK* F: AAACCCAAGGGTAAACAGGA, *MELK* R: ACAGTATGCCATGCTCAA, *PLP2* F: GACCTGCACAC CAAGATACCAT, *PLP2* R: CAAGGACAACAATGGAGGT GAT, *HPRT* F: TGAGGATTGGAAAGGGTGT and *HPRT* R: GAGCACACAGAGGGCTACAA.

Sybr Green I amplification mixtures (12 μL) contained 3 μL of cDNA, 6 μL of 2× Sybr Green I Master Mix (Applied Biosystems, Foster City, CA) and forward and reverse primers at a final concentration 200–400 nM. Reactions were run on an ABI 7500 Real-Time PCR System (Applied Biosystems). The equation $2^{-\Delta\Delta Ct}$ was applied to calculate the relative expression of tumor samples versus the median of nonneoplastic tissues.¹³ All primers were synthesized by IDT (Integrated DNA Technologies, Coralville, IA).

MELK gene copy number quantification

To determine the gene amplification status of *MELK*, QT-PCR was performed using tissue DNA from the same casuistic used for analysis of relative expression. A single copy gene, hemoglobin beta (*HBB*) gene was used as reference. Primer sequences (IDT) were as follows (5'-3'): *MELK* intron 7 F: GCTTTCGACAA TTCTGTGA and *MELK* exon 8 R: ACAGTATGCCATGCTC CAA, *HBB* F: GTGAAGGCTCATGGCAAGA and *HBB* R: AGC TCACTCAGTGTGGCAAAG. Power Sybr Green I Master Mix (Applied Biosystems), DNA and primers (600 nM) were used for gene amplification analysis in QT-PCR reaction mixtures (12 μL). The relative amount of *MELK* with respect to the control gene DNA yield, *HBB*, was calculated using the equation $\Delta Ct = Ct_{HBB} - Ct_{MELK}$, compared to values of nonneoplastic samples. Samples with ΔCt values over 2.0 were considered as having amplification.

MELK promoter methylation analyses

Genomic DNA extracted from 2 nonneoplastic brain samples, 1 PA, 2 low-grade astrocytomas, 1 anaplastic astrocytoma and 5 GBM was subjected to bisulfite treatment to modify unmethylated cytosine to uracil as described previously.¹⁴ The region selected for methylation analyses comprises 39CpG dinucleotides and is located at –201 to +169, from the transcription start site (+1) of the *MELK* gene. Bisulfite-treated DNA was amplified by a nested-PCR protocol using the following primers (5'-3'): *MELK* F: GGTAAGATTAAGGTTAACGTTA and *MELK* R: CTT AACCTAAACACCTCTTC, for the first reaction and *MELK* FN: AGATTAAGGTTAACGTTAAC for the second reaction. PCR was performed in a volume of 25 μL containing 1× PCR buffer, 1.5 mM of MgCl₂, 200 μM dNTPs, 0.32 μM of each

primer and 1 U of Taq Platinum DNA Polymerase (Invitrogen). Amplified products were gel purified and ligated to T-Easy Vector cloning system (Promega, Madison, WI). Six positive clones were sequenced for each sample. DNA sequencing reactions were performed using the Big DyeTM Terminator Cycle Sequencing Ready Reaction Kit version 3.1 (Applied Biosystems) and an ABI Prism 3100 automated sequencer (Applied Biosystems).

MELK RNA interference

siGENOME SMART pool were obtained from Dharmacon Research (Lafayette, CO) and diluted according to manufacturer's protocol. Human glioma cell lines were transfected with *MELK* or nontargeting siRNAs, using Lipofectamine 2000 (Invitrogen). Specific silencing of target gene was confirmed by QT-PCR, at indicated time points.

Assessment of apoptosis

Samples of 1×10^5 cells were washed in phosphate-buffered saline and incubated with 5 μL of PI and annexin-V-FITC solutions (BD, San Diego, CA) for 15 min in the dark to assess cell membrane integrity and exposure of phosphatidylserine residues, respectively. Fluorescence was measured by flow cytometry (FACSCalibur; BD).

Anchorage-independent growth in soft agar

A total of 5×10^3 cells transfected with *MELK*-specific or non-targeting siRNA pools were plated in 0.35% agar/1× DMEM over a layer of 0.5% agar/1× DMEM on 6-well plates. The immobilized cells were grown for 14–21 days in the presence of DMEM supplemented with 10% FCS in a humidified chamber at 37°C with 5% CO₂. Plates were stained with 0.005% crystal violet, and the number and size of the colonies were registered.

Cell proliferation assay

For analysis of cell proliferation, cells transfected with *MELK*-specific or nontargeting siRNA were seeded in a 96-well plate (6,000 cells/well). Nontransfected cells were used as a negative control. Proliferative activity was determined by the MTT (3-(4,5-dimethylthiazol-2-yl)-2,5-diphenyltetrazolium bromide) assay. The absorbance of each well was measured at 580 nm on a microplate reader.

MELK expression in normal tissues

cDNAs were prepared from RNAs from normal tissues (Ambion, Austin, TX; and BD Biosciences, Palo Alto, CA). For QT-PCR, cDNA samples were run in duplicate for *MELK* and for *ACTB* as the reference gene within the same experiment using Taqman platform in the Applied Biosystem apparatus 7500 Fast Real-Time PCR system, PCR primers and probes and the Taqman fast universal PCR mix (Applied Biosystems). PCR conditions were 95°C for 10 min followed by 40 cycles at 95°C for 15 sec and 60°C for 1 min. Relative quantification of gene expression was determined using the equation $2^{-\Delta\Delta Ct}$.¹³ Bladder tissue was used as reference.

Statistical analysis

The statistical analysis of relative gene expression in different grades of astrocytomas and nonneoplastic tissues was assessed using the Mann-Whitney test and the analyses of anchorage-independent growth in soft agar of malignant astrocytomas cell lines was performed by Student's *t*-test (nonparametric). Differences were considered to be statistically significant at $p < 0.05$. Overall survival was calculated as the interval between day of surgery and day of death, in months. Patients alive on the day of analysis were censored on December 9, 2006. Calculations were performed using SPSS 10.0 software (SPSS, Chicago, IL).

Results

Identification of genes exhibiting higher levels of expression in astrocytomas than nonneoplastic brain tissues by microarray analysis

Microarray analyses were undertaken using cDNA prepared from 3 PA (Grade I), 6 GBM (Grade IV) and 2 pools of 3 nonneoplastic brain tissue samples. In all pair-wise comparisons, the average of the coefficients of variation for duplicates ranged from 6.5 to 9.0%, with Pearson correlation coefficients being higher than 0.98. For all duplicates, more than 99.7% of the values were within a 2-fold difference.

Similar numbers of genes, 562 and 555, were found to be at least 2-fold overexpressed in the GBM and PA samples as compared to the pooled nonneoplastic tissues, respectively. Of these, 319 were overexpressed genes in both tissues. However, in a comparison of each of the GBM and PA samples in a pair-wise fashion, only 63 genes were found to have at least a 2-fold higher level of expression in all GBM samples as compared to the PA samples.

A functional classification of the GBM overexpressed genes revealed that 40% are related to the cell cycle and mitosis (Table I). Several of these genes have been reported to be associated with cellular transformation and increased malignancy in a number of different cancer types including gliomas,^{15–18} as indicated in Table II. It is noteworthy that other microarray studies have consistently identified *CDC20*, *UBE2C*, *PCNA*, *KIAA0101* and *BIRC5* as markers of malignancy.

The microarray data were validated by QT-PCR for 6 of the genes with the highest relative overexpression in GBM relative to PA: *MELK*, *AUKB*, *ASPM*, *PRC1*, *IL13RA2* and *KIAA0101* (Fig. 1). In all cases, the PCR measurements demonstrated a clear average increase in expression in GBM as compared with PA, although in 4 of the 6 the overlap between the levels of expression exhibited by the 2 tumor types (*AUKB*, *PRC1* and *IL13RA2*) resulted in the differential expression not being statistically significant. However, the expression of *KIAA0101*, *ASPM* and *MELK* was sufficiently high in the 13 GBM samples assayed and that statistical significance was maintained. The finding of the consistent high level of expression of *MELK* in aggressive glioblastomas was of interest given that as a kinase it is likely to be druggable and also since it has been recently identified as a potential therapeutic target on the basis of its overexpression in a number of cancer types.⁹ Moreover, it has been demonstrated to be a key regulator of the proliferation of multipotent neural progenitors.¹⁰ Therefore, among these genes selected from the analysis of the microarray data, we elected to characterize the expression of *MELK* in more detail and investigate whether it might be directly related to the malignant properties of GBM as has been shown in cell lines derived from other cancer types.

MELK expression correlates with tumor grade

As a first step, we measured *MELK* mRNA levels by QT-PCR in an extended series of tumor samples including both Grade II and Grade III astrocytomas as well as medulloblastomas. We confirmed in this larger data set the consistent and high levels of *MELK* expression in Grade IV GBMs (645-fold that of normal tissues) with just 2 of the 53 samples studied exhibiting aberrantly low levels of expression similar to that found in normal tissues. The Grade II and Grade III tumors were found to exhibit progressively higher levels of *MELK* expression (162- and 221-fold, respectively) as compared to nonneoplastic samples. The median expression level of *MELK* was 88.2-fold higher in PA than normal tissues, thus overall demonstrating an increase in *MELK* expression in parallel to the increase in malignancy (Fig. 2a). *MELK* expression levels in medulloblastoma were similar to GBM. It should be noted that this association of gene expression with tumor grade was not typical and that the majority of genes that are upregulated in GBM are similarly upregulated in PA as illustrated here for *PLP2* (Fig. 2b). We found no direct relationship between *MELK* expression level in GBM and survival time by Kaplan-

TABLE I – GENES OVEREXPRESSED IN GLIOBLASTOMA RELATIVE TO PILOCYTIC ASTROCYTOMA, MEASURED BY MICROARRAY ANALYSIS

| Accession no. | Description | Locus | Mean-fold change |
|--------------------------------------|--|-------------|------------------|
| Cell proliferation | | | |
| NM_001255 | CDC20 cell division cycle 20 homolog (<i>S. cerevisiae</i>) (<i>CDC20</i>) | 1p34.1 | 20.07 |
| NM_004217 | Aurora kinase B (<i>AURKB</i>) | 17p13.1 | 16.1 |
| NM_002497 | NIMA (never in mitosis gene a)-related kinase 2 (<i>NEK2</i>) | 1q32.2–41 | 15.72 |
| NM_001809 | Centromere protein A, 17 kDa (<i>CENPA</i>) | 2p24–21 | 13.68 |
| NM_001657 | Amphiregulin (Schwannoma-derived growth factor) (<i>AREG</i>) | 4q13–21 | 11.2 |
| NM_001786 | Cell division cycle 2, G1 to S and G2 to M (<i>CDC2</i>) | 10q21.1 | 9.76 |
| NM_006845 | Kinesin family member 2C (<i>KIF2C</i>) | 1p34.1 | 8.66 |
| NM_001827 | CDC28 protein kinase regulatory subunit 2 (<i>CKS2</i>) | 9q22 | 7.95 |
| NM_002358 | MAD2 mitotic arrest deficient-like 1 (yeast) (<i>MAD2L1</i>) | 4q27 | 7.77 |
| NM_001813 | Centromere protein E, 312 kDa (<i>CENPE</i>) | 4q24–25 | 7.7 |
| NM_031966 | Cyclin B1 (<i>CCNB1</i>) | 5q12 | 7.08 |
| NM_016343 | Centromere protein F, 350/400 kDa (mitosin) (<i>CENPF</i>) | 1q32–41 | 7.06 |
| NM_003981 | Protein regulator of cytokinesis 1 (<i>PRC1</i>) | 15q26.1 | 6.66 |
| NM_003318 | TTK protein kinase (<i>TTK</i>) | 6q13–21 | 6.38 |
| NM_022346 | Chromosome condensation protein G (<i>NCAPG</i>) | 4p15.33 | 6.11 |
| NM_012112 | TPX2, microtubule-associated protein homolog (<i>Xenopus laevis</i>) (<i>TPX2</i>) | 20q1.2 | 5.96 |
| NM_003035 | TAL1 (SCL) interrupting locus (<i>STIL</i>) | 1p32 | 4.22 |
| NM_001237 | Cyclin A2 (<i>CCNA2</i>) | 4q25–31 | 3.78 |
| Cell proliferation/DNA damage | | | |
| NM_000597 | Insulin-like growth factor binding protein 2, 36 kDa (<i>IGFBP2</i>) | 2q33–34 | 18.14 |
| NM_001274 | CHK1 checkpoint homolog (<i>S. pombe</i>) (<i>CHK1</i>) | 11q24–24 | 9.55 |
| NM_199420 | Polymerase (DNA directed), θ (<i>POLQ</i>) | 3q13.33 | 8.9 |
| NM_022809 | Cell division cycle 25C (<i>CDC25C</i>) | 1p34.1 | 8.61 |
| NM_001827 | CDC28 protein kinase regulatory subunit 2 (<i>CKS2</i>) | 9q22 | 7.95 |
| NM_002875 | RAD51 homolog (RecA homolog, <i>E. coli</i>) (<i>S. cerevisiae</i>) (<i>RAD51</i>) | 15q15.1 | 7.01 |
| NM_002592 | Proliferating cell nuclear antigen (<i>PCNA</i>) | 20pter–12 | 2.72 |
| DNA and protein metabolism | | | |
| NM_007019 | Ubiquitin-conjugating enzyme E2C (<i>UBE2C</i>) | 20q13.12 | 17 |
| NM_014791 | Maternal embryonic leucine zipper kinase (<i>MELK</i>) | 9p13.2 | 16.45 |
| NM_002317 | Lysyl oxidase (<i>LOX</i>) | 5q23.3–31.2 | 11.04 |
| NM_003294 | Tryptase $\alpha/\beta 1$ (<i>TPSAB1</i>) | 16p13.3 | 8.99 |
| NM_014176 | HSPC150 protein similar to ubiquitin-conjugating enzyme (<i>UBE2T</i>) | 1q32.1 | 7.85 |
| NM_018518 | MCM10 minichromosome maintenance deficient 10 (<i>S. cerevisiae</i>) (<i>MCM10</i>) | 10p13 | 6.3 |
| NM_000943 | Peptidylprolyl isomerase C (cyclophilin C) (<i>PPIC</i>) | 5q23.2 | 5.31 |
| NM_001071 | Thymidylate synthetase (<i>TYMS</i>) | 18p11.32 | 4.26 |
| NM_030928 | DNA replication factor (<i>CDT1</i>) | 16q24.3 | 3.76 |
| Transcription | | | |
| NM_019102 | Homeobox protein (<i>HOXA5</i>) | 7p15–14 | 16.97 |
| NM_006897 | Homeobox C9 (<i>HOXC9</i>) | 12q13.3 | 8.29 |
| NM_004237 | Thyroid hormone receptor interactor 13 (<i>TRIP13</i>) | 5p13.33 | 7.34 |
| BC033086 | Transcription factor 19 (SC1) (<i>TCF19</i>) | 6q21.3 | 6.09 |
| Cell adhesion | | | |
| NM_019119 | Protocadherin $\beta 9$ (<i>PCDHB9</i>) | 5q31 | 9.81 |
| NM_004369 | Collagen, type VI, $\alpha 3$ (<i>COL6A3</i>) | 2q27 | 6.47 |
| Signal transduction/receptors | | | |
| NM_000640 | Interleukin 13 receptor, $\alpha 2$ (<i>IL13RA2</i>) | Xq13.1–28 | 32.62 |
| NM_001999 | Fibrillin 2 (congenital contractual arachnodactyly) (<i>FBN2</i>) | 5q23–31 | 13.61 |
| NM_006681 | Neuromedin U (<i>NMU</i>) | 4q12 | 11.75 |
| NM_018154 | ASF1 antisilencing function 1 homolog B (<i>S. cerevisiae</i>) (<i>ASF1B</i>) | 19p13.12 | 9.78 |
| NM_007280 | Opa-interacting protein 5 (<i>OIPS5</i>) | 15q15.1 | 7.2 |
| NM_000599 | Insulin-like growth factor binding protein 5 (<i>IGFBP5</i>) | 2q33.q36 | 7.16 |
| NM_018098 | Epithelial cell transforming sequence 2 oncogene (<i>ECT2</i>) | 3q26.1–26.2 | 5.8 |
| NM_005497 | Gap junction protein, $\alpha 7$, 45 kDa (connexin 45) (<i>GJA7</i>) | 17q21.31 | 5.29 |
| NM_006863 | Leukocyte immunoglobulin-like receptor, subfamily A, member 1 (<i>LILRA1</i>) | 19q13.4 | 3.09 |
| Angiogenesis/defense | | | |
| NM_000584 | Interleukin 8 (<i>IL8</i>) | 4q13–21 | 7.11 |
| NM_000636 | Superoxide dismutase 2, mitochondrial (<i>SOD2</i>) | 6q25.3 | 5.75 |
| Cytoskeleton | | | |
| NM_001456 | Filamin A, α (actin binding protein 280) (<i>FLNA</i>) | Xq28 | 4.47 |
| NM_002705 | Periplakin (<i>PPL</i>) | 16p13.1 | 3.57 |
| Apoptosis inhibitors | | | |
| NM_001168 | Baculoviral IAP repeat-containing 5 (<i>BIRC5</i>) | 17q25 | 16.46 |
| Organogenesis | | | |
| NM_001849 | Collagen, type VI, $\alpha 2$ (<i>COL6A2</i>) | 21q22.3 | 11.46 |
| Unknown function | | | |
| NM_018136 | Asp (abnormal spindle)-like, microcephaly associated (<i>Drosophila</i>) (<i>ASPM</i>) | 1q31 | 16.88 |
| NM_014736 | KIAA0101 gene product (<i>KIAA0101</i>) | 15q22.31 | 13.98 |
| NM_018410 | Hypothetical protein (<i>DKFZp762E1312</i>) | 2q37.1 | 9.2 |
| NM_182487 | Olfactomedin-like 1A (<i>OLFML2A</i>) | 9q33.3 | 8.02 |
| NM_018455 | Uncharacterized bone marrow protein BM039 (<i>CENPN</i>) | 16q23.2 | 4.69 |
| NM_018454 | Nucleolar protein ANKT (<i>NUSAPI</i>) | 15q15.1 | 4.56 |
| NM_030804 | Hypothetical protein DKFZp434E2135 (<i>FZD5</i>) | 2q33–34 | 3.88 |
| NM_015426 | DKFZP434C245 protein (<i>WDR51A</i>) | 3p21.1 | 3.56 |

TABLE II – COMPARISON BETWEEN GBM VERSUS PA DIFFERENTIALLY EXPRESSED GENES

| Type of assay | Total genes | Genes in common to our GBM vs. PA | Reference |
|--|-----------------|---|-----------|
| cDNA microarray (6,800 genes, 21 grade IV vs. 9 grade I astrocytoma tissues) | 133 | <i>CKS2, CDC20, BIRC5, UBE2C, PCNA, FLNA, CENPA, KIAA0101, IL13RA2, CCNB1, KIF2C, CENPF, MELK</i> | 17 |
| Comparative meta-profiling of 40 microarray data sets (3,762 microarrays) | 43 ¹ | <i>CDC20, UBE2C, PCNA, BIRC5, KIAA0101, CENPA, MELK, KIF2C, CKS2</i> | 16 |
| cDNA microarray (12,000 genes, 6 grade IV vs. grade I astrocytoma) | 15 | <i>IGFBP2</i> | 18 |
| Suppression subtractive hybridization (648 clones GBM vs. 648 PA) | 32 | None | 19 |

¹43 common overexpressed genes comparing high- and low-grade lung adenocarcinoma, bladder carcinoma, breast ductal carcinoma, glioma, ovarian carcinoma, prostate carcinoma.

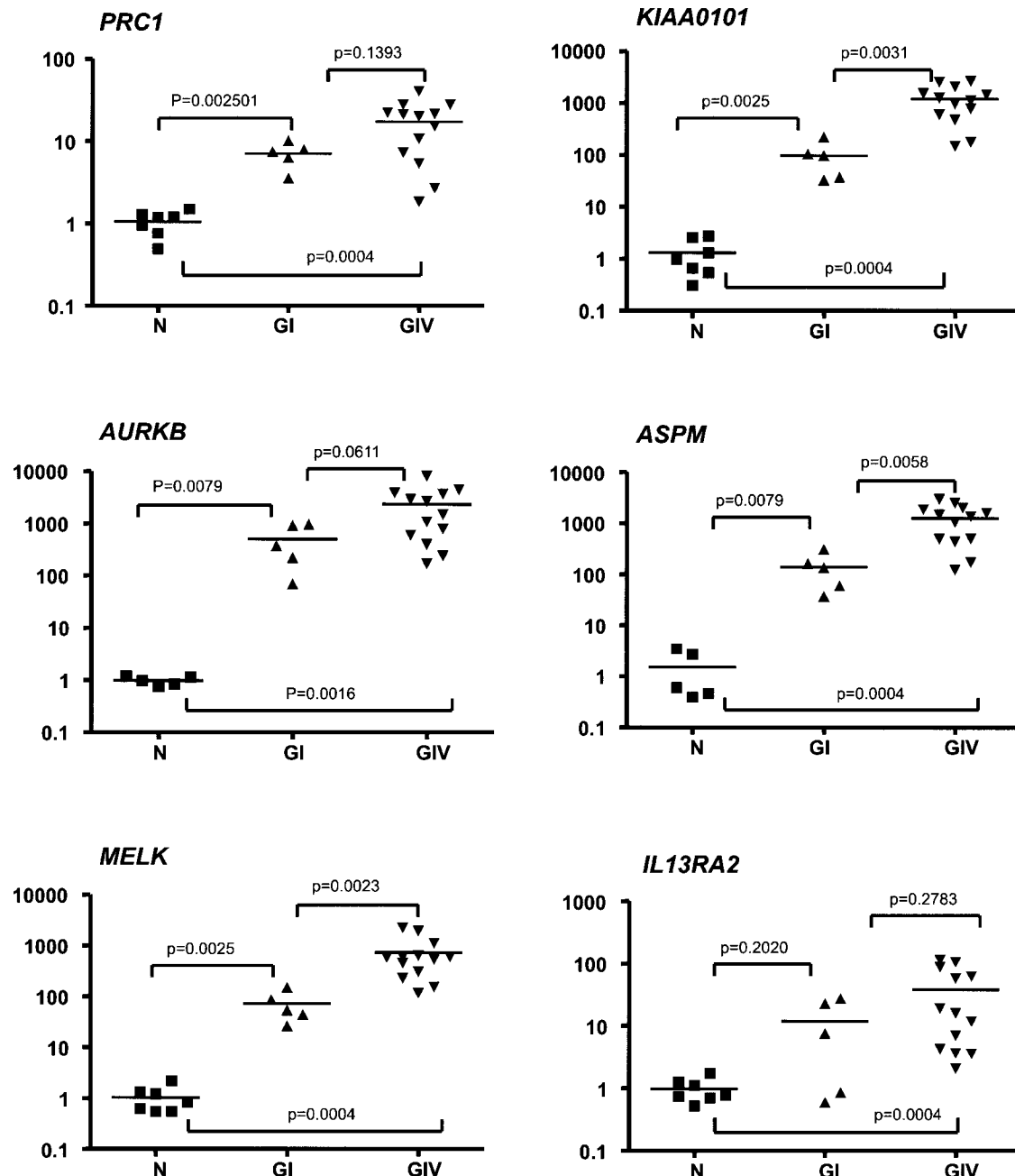


FIGURE 1 – Expression levels of putative tumor markers in astrocytomas. Transcript levels for *KIAA0101*, *PRC1*, *AURKB*, *ASPM*, *MELK* and *IL13RA2* were determined by quantitative real-time PCR in 7 nonneoplastic brain samples (N), 5 pilocytic astrocytomas (GI) and 13 glioblastomas (GIV). Relative expression values were calculated based on the *HPRT* expression levels of each sample and nonneoplastic brain values. The horizontal bars show the median of each group, and the statistical p values according to Mann-Whitney test are shown for each comparison.

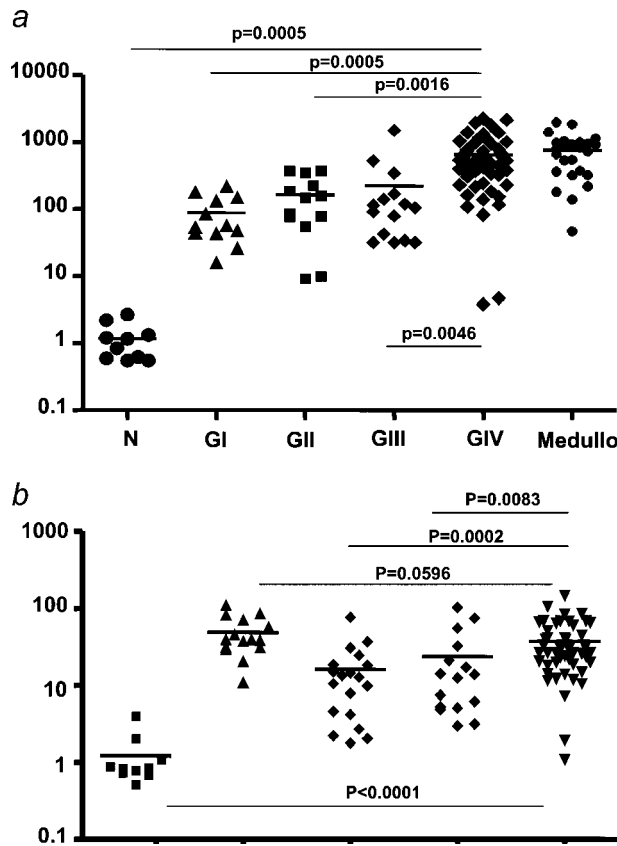


FIGURE 2 – mRNA expression levels of (a) *MELK* and (b) *PLP2* in tumor and nonneoplastic tissues. Different grades of astrocytoma (pilocytic astrocytomas, GI; low-grade astrocytomas, GII; anaplastic astrocytomas, GIII; glioblastomas, GIV), nonneoplastic (N) and medulloblastoma (Medullo) tissues were reverse transcribed and cDNAs were analyzed by QT-PCR. Expression levels ($\log 10 \times 2^{-\Delta\Delta Ct}$) were calculated based on *HPRT* expression levels of each sample. The horizontal bar shows the median of each group, and the significance values according to Mann-Whitney test are shown at each comparison.

Meier analysis (log rank $p = 0.455$), which probably reflects the relatively uniform expression of the gene in tumors (data not shown).

Lack of evidence for *MELK* promoter hypomethylation or gene amplification

The phenomenon of very low level expression of embryonic genes in adult tissues and their upregulation in tumors can be due to promoter hypermethylation in normal tissues that is reversed during tumorigenesis. We examined this possibility for *MELK* and identified a CpG island (39 CpG dinucleotides) located at nucleotides -201 to +169 in relation to the transcription start site (+1). Methylation status in this island was measured by sequencing bisulfite-modified DNA, but no difference was found in the promoter methylation profile in the bisulfite-treated DNA from astrocytic tumor tissues (1 PA, 2 low-grade astrocytomas, 1 anaplastic astrocytoma and 5 GBM samples) and 2 nonneoplastic tissues as controls (data not shown). All samples analyzed, including the nonneoplastic tissues, presented a completely unmethylated profile in each of the 6 clones analyzed. We also asked whether gene upregulation might be accompanied by gene amplification, which is the case for a number of oncogenes. However, no *MELK* gene amplification was found by QT-PCR in 93 DNA astrocytoma samples with different grades of malignancy as compared with normal tissues (data not shown).

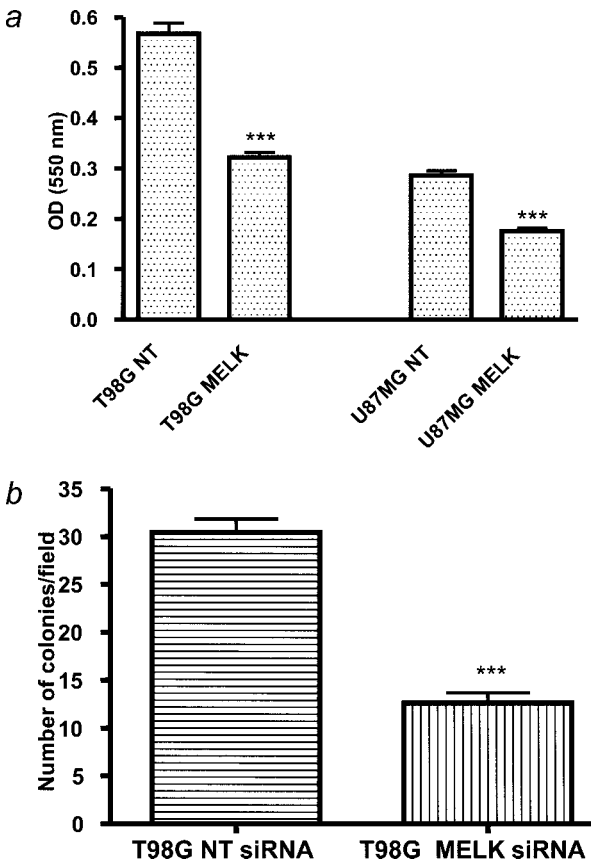


FIGURE 3 – Effect of *MELK* downregulation on *in vitro* behavior of malignant astrocytoma cell lines. (a) Effect on cell proliferation as measured by MTT assay on the fourth day following transfection with nontargeting (NT) or *MELK*-specific siRNA pools using T98G and U87MG cell lines. (b) Effect of *MELK* knock-down on anchorage-independent growth as measured by colony formation assays. The T98G cell line transfected with *MELK*-specific siRNA pool showed reduced capacity to form colonies in soft agar compared with negative controls. The mean and standard error of the mean (SEM) were calculated from 6 replicates for the MTT assay and from 20 fields in 2 separate wells for the colony formation assay. Statistically significant differences from control are indicated as *** ($p < 0.001$). Similar results were obtained from 2 independent experiments.

MELK depletion by siRNA results in apoptosis-dependent growth inhibition in glioma cell lines and reduced clonogenicity

There is evidence that *MELK* can directly influence proliferation and anchorage-independent growth, but this has not yet been established in the context of GBM. To investigate this possibility, we used small interference RNAs (siRNAs) to reduce *MELK* mRNA levels in 2 malignant astrocytoma cell lines (T98G and U87MG). This procedure had the effect of reducing *MELK* expression levels by up to 95%. This effect on *MELK* mRNA was apparently specific, since the nontargeting control (NT) had no effect and was sustained for at least 7 days posttransfection, when approximately a 65% knockdown was still detectable (data not shown). The treatment of both U87MG and T98G with *MELK*-specific siRNA pools resulted in a reduction in cell proliferation (Fig. 3a). This was accompanied by a modest but significant increase of cleaved caspase-3 positive cells ($p < 0.01$) or annexin V-stained cells ($p < 0.05$), as detected by FACS analysis on days 2 and 7 (data not shown), suggesting that the observed alterations in growth kinetics was, at least in part, due to enhanced apoptosis.

Anchorage-independent growth assays were next used to examine the influence of *MELK* on colony formation. Both T98G and U87MG cell lines were transfected with siRNA against *MELK* or

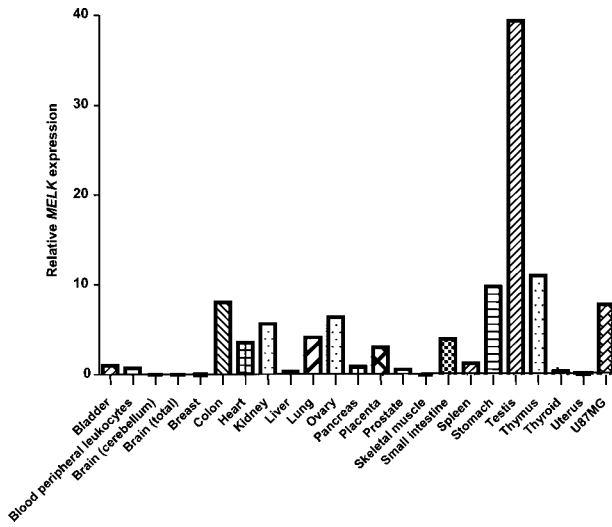


FIGURE 4 – MELK expression in normal tissues. Quantitative real time PCRs were performed with c-DNA samples prepared from RNAs from several normal tissues for *MELK* and *ACTB* used as an endogenous control gene. The cDNA templates used were normalized on the basis of *ACTB* amplification.

nontargeting siRNA and, as shown in Figure 3b, this resulted in reduced colony formation on soft agar by the T98G cells. A reduction in colony number was not observed with the U87MG cells, although they did exhibit a 30% relative reduction in size as compared with controls over the time period of the experiment (data not shown). Overall, these results show that this level of inhibition on *MELK* expression is sufficient to partially modulate tumor growth.

Quantitative analysis of *MELK* expression in normal tissues

Given the emerging evidence of the importance of *MELK* in astrocytoma malignancy, and hence its potential utility as a therapeutic target, we assessed its expression in a variety of normal tissues by QT-PCR (Fig. 4). The apparent absence of *MELK* expression in normal brain is consistent with the data presented earlier and encouraging in terms of its utility as a target. However, there were significant levels of expression detectable in gastrointestinal tissues that would have to be taken into account in the potential utilization of *MELK* inhibitors as a cancer treatment.

Discussion

GBM is resistant to conventional therapies and survival time is usually shorter than 12 months. Therefore, the identification of additional molecular alterations involved in the establishment of the aggressive behavior of astrocytic tumors, and that can be targeted by pharmacological agents, is a critical challenge. A number of targetable genetic changes have been described in human gliomas, such as *EGFR* overexpression/amplification and activation of tyrosine kinase receptors, but they are not applicable to all tumors.^{18,20}

Genome-wide analysis of gene expression is a powerful and widely used approach for identifying therapeutic targets for cancer treatment.^{11,15,17,19–23} However, comparison of global expression profiles of normal and tumor cells usually generates hundreds of differentially expressed genes in cancer relative to normal tissue, most of them probably not playing critical roles in the tumorigenic process. For this reason, we decided to compare PA, a noninvasive indolent tumor with GBM, which is highly invasive and rapidly lethal, with the hope of identifying genes directly involved in malignancy. When either GBM or PA were compared to nonneoplastic brain tissues, over 500 genes were found differentially expressed

in each case. When GBM was compared to PA, on the other hand only 63 genes were found to have at least a 2-fold different level of expression between these tumor types. Several groups have analyzed the profile of proliferation in various cancer types including gliomas and Table II shows a list of genes in common between our array and published data. Rickman *et al.*¹⁷ found 167 genes overexpressed in a molecular profile study of high-grade (GBM) and low-grade (PA) gliomas based on oligonucleotide microarray analysis; among those, we also found 7 exhibiting differential expression between GBM and PA: *CKS2*, *CDC20*, *IGFBP2*, *IAP4*, *UBE2C*, *PCNA* and *FLNA*. Khatua *et al.*¹⁸ also compared high-grade astrocytomas versus benign low-grade pediatric astrocytomas using a DNA microarray and found 17 overexpressed genes, *IGFBP2* among them. Tso *et al.*²⁴ have compared primary and secondary GBM to astrocytomas and found 12 genes in common to our list, including *CENPF*, *CDC2*, *UBE2C*, *CKS2*, *ECT2*, *ASPM*, *PRC1*, *COL6A2*, *IL8*, *SOD2*, *LOX* and *IGFBP2*. Rhodes *et al.*¹⁶ used a large-scale meta-analysis of several cancer microarrays data and identified *CDC20*, *UBE2C*, *CKS2*, *KIF2C*, *BIRC5*, *KIAA0101*, *CENPA* and *MELK* among 43 genes that form a common transcriptional profile of human cancer. On the other hand, our results showed no overlap with the list of genes generated by Colin *et al.*¹⁹ using Suppression Subtractive Hybridization method to compare differentially expressed genes in GBM versus PA, possibly because of significant differences in the methodology.

In this study, we selected genes among the highly expressed in GBM compared to PA, expecting that they were related not only to the tumorigenic process itself, but also to increase of malignancy. We noted that most (>50%) of the genes in our list were related to cell proliferation, acting directly in the cell cycle, and proliferating cell nuclear antigen, or that function in the regulation or assembly of the mitotic spindle.

Additionally, among the most highly expressed genes in GBM in relation to PA we found interleukin-13 receptor α -2 (*IL13RA2*)^{25–29} and other putative tumor marker genes, such as the *HOX* genes, which have been associated with different cancer types.^{30–32}

An ancillary contribution of this study is the generation of functional data for somewhat uncharacterized human genes. Among them, we have detected *KIAA0101* that encodes a proliferating cell nuclear antigen (PCNA)-interacting protein named p15 (PAF), as 13.98-fold increased in GBM compared to PA. Its expression has been described as downregulated in human hepatocellular carcinoma³³ but upregulated in several other tumors.^{34,35} The contribution of such uncharacterized proteins to the malignancy of astrocytomas and their relevance to prognosis and therapy is worth of further investigation.

Among the overexpressed genes in GBM, we selected *MELK* as being of particular interest. Although this gene has received relatively little attention in the context of human malignancy until recently, it is emerging as an important and possibly ubiquitous contributor to this process. We noted here that its expression correlated with grade of malignancy and exhibited an almost uniformly high level of expression in GBM and medulloblastoma. This stands in contrast to the range of levels of expression of other key genes in GBM such as *EGFR*.³⁶ Only 2 out of 53 GBM patients presented *MELK* expression overlapping to the expression of nonneoplastic brain tissue. These 2 patients were submitted to tumor resection surgery at 50 and 71 years of age, and survived for 7 and 2 months, respectively. Thus the reason for their low expression of *MELK* is not obvious. This homogeneous aspect of expression among GBM and medulloblastoma potentially represents an advantage for the use of *MELK* as a therapeutic target. In this regard, we were able to directly demonstrate that *MELK* functions in the context of human astrocytomas, by knockdown of its expression by RNA interference in malignant astrocytoma cell lines. As a result, growth-inhibition, as determined by the MTT cell proliferation assay, as well a decrease in anchorage-independent

ent colony formation were observed. The antiproliferative effect of *MELK* has been demonstrated *in vitro* experiments, which have confirmed *MELK* as the transcriptional repressor E2F target.³⁷

Furthermore, we noted here a modest but significant increase in both caspase-3 expression and in annexin-V-staining indicating a role in inhibiting apoptosis in malignant astrocytoma cells. Animal experiments have indicated that *MELK* plays a role in the control of apoptosis acting through zinc-finger-like protein 9 (ZPR9).^{38,39} More recently, it has been reported in breast cancer cell lines that *MELK* interacts with members of the Bcl-2 family of proapoptotic genes, Bcl-G_L, leading to its phosphorylation and suppression of apoptosis.⁴⁰

In addition to ZPR9, other *MELK* interacting proteins include NIPPI⁴¹ and CDC25B.⁴² Examination of our microarray data indicate that the expression of these genes may be coordinated with that of *MELK*, in that ZPR622 (NM_033414.2, corresponding to ZPR9) exhibited a 0.49 mean fold change of expression in GBM as compared to nonneoplastic brain tissue, and similarly *B-MYB* (NM_002466.2) presented a ratio of 0.28. In contrast, *NIPPI* (protein phosphatase 1, regulatory-inhibitor- subunit 8 transcript variant 1, NM_014110.3) and *CDC25B* (cell division cycle 25B, transcript variant 5, NM_212530.1) presented, respectively, 7.55 and 7.31 mean-fold change in GBM compared to nonneoplastic brain tissue.

MELK is a protein Ser/Thr kinase implicated in cell cycle progression. In the context of human cancer, *MELK* expression has been observed to be significantly lower in growth-arrested nonmalignant human mammary epithelial cells that form organized polarized acini *in vitro* than in their proliferating counterparts, thus corroborating its role in the proliferative process. This attribute allowed the use of *MELK* expression as a marker to classify breast cancer patients into groups of differential prognosis.⁴³ *MELK* has been implicated in the control of cell proliferation during development⁴⁴ being found enriched in embryonic and adult

neural stem/progenitor cells and required for their self-renewal capacity.^{10,45} Deregulation of the molecular pathways governing stem cell-like behavior in cancer cells may be critical for the development of new strategies for cancer prevention and therapy. The increased expression of *MELK* in the CD133 positive compartment of gliomas, as demonstrated by our experiments,⁴⁶ and by others,⁴⁷ may indicate that *MELK* overexpression is a hallmark of cancer stem cells, and that targeting *MELK* activity in cancer stem cells may thus be useful to increase the efficacy of GBM treatment.

In conclusion, the striking contrast in clinical and pathological behavior between GBM and PA is associated with a rather limited divergence at the gene expression level, with transcripts for protein involved mainly in cell proliferation accounting for the main differences. These findings provide additional information concerning the molecular nature of astrocytomas of distinct grades of malignancy, which ultimately may contribute towards improving tumor classification and therapeutic strategies. Among these differentially expressed genes, we have found that *MELK* expression correlates with the malignant grade of human astrocytic tumors. The effects of *MELK* silencing on proliferation, apoptosis and anchorage independent growth of malignant astrocytic cells suggest that *MELK* deregulation may contribute to the malignant progression of this tumor type, and further support the hypothesis that it might represent a useful target for novel therapeutic agents for treating human glioblastomas.

Acknowledgements

The authors are grateful to Dr. Paulo Henrique de Aguiar, Dr. Flavio Miura, Dr. Edson Nakagawa, Dr. Hamilton Matsushita for collecting samples during surgical procedure; Dr. Ricardo Pereira Moura for the methylation assays; Dr. Juçara Parra for administrative support; and Mrs. Erika Ritter.

References

1. Kleihues P, Louis DN, Scheithauer BW, Rorke LB, Reifenberger G, Burger PC, Cavenee WK. The WHO classification of tumors of the nervous system. *J Neuropathol Exp Neurol* 2002;61:215–25; discussion 226–9.
2. von Deimling A, Louis DN, Schramm J, Wiestler OD. Astrocytic gliomas: characterization on a molecular genetic basis. *Recent Results Cancer Res* 1994;135:33–42.
3. Korshunov A, Sycheva R, Golovan A. The prognostic relevance of molecular alterations in glioblastomas for patients age <50 years. *Cancer* 2005;104:825–32.
4. von Deimling A, Louis DN, Wiestler OD. Molecular pathways in the formation of gliomas. *Glia* 1995;15:328–38.
5. Brentani H, Caballero OL, Camargo AA, da Silva AM, da Silva WA, Jr, Dias Neto E, Grivet M, Gruber A, Guimaraes PE, Hide W, Iseli C, Jongeneel CV, et al. The generation and utilization of a cancer-oriented representation of the human transcriptome by using expressed sequence tags. *Proc Natl Acad Sci USA* 2003;100:13418–23.
6. Velculescu VE, Zhang L, Vogelstein B, Kinzler KW. Serial analysis of gene expression. *Science* 1995;270:484–7.
7. Jongeneel CV, Iseli C, Stevenson BJ, Riggins GJ, Lal A, Mackay A, Harris RA, O'Hare MJ, Neville AM, Simpson AJ, Strausberg RL. Comprehensive sampling of gene expression in human cell lines with massively parallel signature sequencing. *Proc Natl Acad Sci USA* 2003;100:4702–5.
8. Grigoriadis A, Mackay A, Reis-Filho JS, Steele D, Iseli C, Stevenson BJ, Jongeneel CV, Valgeirsson H, Fenwick K, Iravani M, Leao M, Simpson AJ, et al. Establishment of the epithelial-specific transcriptome of normal and malignant human breast cells based on MPSS and array expression data. *Breast Cancer Res* 2006;8:R56.
9. Gray D, Jubb AM, Hogue D, Dowd P, Kljavin N, Yi S, Bai W, Frantz G, Zhang Z, Koeppen H, de Sauvage FJ, Davis DP. Maternal embryonic leucine zipper kinase/murine protein serine-threonine kinase 38 is a promising therapeutic target for multiple cancers. *Cancer Res* 2005;65:9751–61.
10. Nakano I, Paukar AA, Bajpai R, Dougherty JD, Zewail A, Kelly TK, Kim KJ, Ou J, Groszer M, Imura T, Freije WA, Nelson SF, et al. Maternal embryonic leucine zipper kinase (MELK) regulates multipotent neural progenitor proliferation. *J Cell Biol* 2005;170:413–27.
11. Oba-Shinjo SM, Bengtson MH, Winnischofer SM, Colin C, Vedoy CG, de Mendonca Z, Marie SK, Sogayar MC. Identification of novel differentially expressed genes in human astrocytomas by cDNA representational difference analysis. *Brain Res Mol Brain Res* 2005;140:25–33.
12. Cavalieri D, De Filippo C. Bioinformatic methods for integrating whole-genome expression results into cellular networks. *Drug Discov Today* 2005;10:727–34.
13. Livak KJ, Schmittgen TD. Analysis of relative gene expression data using real-time quantitative PCR and the 2^{-Delta Delta C(T)} method. *Methods* 2001;25:402–8.
14. Jeronimo C, Usadel H, Henrique R, Silva C, Oliveira J, Lopes C, Sidransky D. Quantitative GSTP1 hypermethylation in bodily fluids of patients with prostate cancer. *Urology* 2002;60:1131–5.
15. Horvath S, Zhang B, Carlson M, Lu KV, Zhu S, Feliciano RM, Laurence MF, Zhao W, Qi S, Chen Z, Lee Y, Scheck AC, et al. Analysis of oncogenic signaling networks in glioblastoma identifies ASPM as a molecular target. *Proc Natl Acad Sci USA* 2006;103:17402–7.
16. Rhodes DR, Yu J, Shanker K, Deshpande N, Varambally R, Ghosh D, Barrette T, Pandey A, Chinnaiyan AM. Large-scale meta-analysis of cancer microarray data identifies common transcriptional profiles of neoplastic transformation and progression. *Proc Natl Acad Sci USA* 2004;101:9309–14.
17. Rickman DS, Bobek MP, Misek DE, Kuick R, Blaivas M, Kurnit DM, Taylor J, Hanash SM. Distinctive molecular profiles of high-grade and low-grade gliomas based on oligonucleotide microarray analysis. *Cancer Res* 2001;61:6885–91.
18. Khattau S, Peterson KM, Brown KM, Lawlor C, Santi MR, LaFleur B, Dressman D, Stephan DA, MacDonald TJ. Overexpression of the EGFR/FKBP12/HIF-2α pathway identified in childhood astrocytomas by angiogenesis gene profiling. *Cancer Res* 2003;63:1865–70.
19. Colin C, Baeza N, Bartoli C, Fina F, Eudes N, Nanni I, Martin PM, Ouafik L, Figarella-Branger D. Identification of genes differentially expressed in glioblastoma versus pilocytic astrocytoma using suppression subtractive hybridization. *Oncogene* 2006;25:2818–26.
20. van den Boom J, Wolter M, Kuick R, Misek DE, Youkilis AS, Wechsler DS, Sommer C, Reifenberger G, Hanash SM. Characterization of gene expression profiles associated with glioma progression using oligonucleotide-based microarray analysis and real-time reverse

- transcription-polymerase chain reaction. *Am J Pathol* 2003;163:1033–43.
21. Sallinen SL, Sallinen PK, Haapasalo HK, Helin HJ, Helen PT, Schraml P, Kallioniemi OP, Kononen J. Identification of differentially expressed genes in human gliomas by DNA microarray and tissue chip techniques. *Cancer Res* 2000;60:6617–22.
 22. Gutmann DH, Hedrick NM, Li J, Nagarajan R, Perry A, Watson MA. Comparative gene expression profile analysis of neurofibromatosis 1-associated and sporadic pilocytic astrocytomas. *Cancer Res* 2002;62:2085–91.
 23. Mischel PS, Cloughesy TF, Nelson SF. DNA-microarray analysis of brain cancer: molecular classification for therapy. *Nat Rev Neurosci* 2004;5:782–92.
 24. Tso CL, Freije WA, Day A, Chen Z, Merriman B, Perlina A, Lee Y, Dia EQ, Yoshimoto K, Mischel PS, Liau LM, Cloughesy TF, et al. Distinct transcription profiles of primary and secondary glioblastoma subgroups. *Cancer Res* 2006;66:159–67.
 25. Liu H, Jacobs BS, Liu J, Prayson RA, Estes ML, Barnett GH, Barna BP. Interleukin-13 sensitivity and receptor phenotypes of human glial cell lines: non-neoplastic glia and low-grade astrocytoma differ from malignant glioma. *Cancer Immunol Immunother* 2000;49:319–24.
 26. Kelly-Welch AE, Hanson EM, Boothby MR, Keegan AD. Interleukin-4 and interleukin-13 signaling connections maps. *Science* 2003;300:1527–8.
 27. Kawakami M, Leland P, Kawakami K, Puri RK. Mutation and functional analysis of IL-13 receptors in human malignant glioma cells. *Oncol Res* 2001;12:459–67.
 28. Mintz A, Gibo DM, Madhankumar AB, Debinski W. Molecular targeting with recombinant cytotoxins of interleukin-13 receptor α 2-expressing glioma. *J Neurooncol* 2003;64:117–23.
 29. Husain SR, Puri RK. Interleukin-13 receptor-directed cytotoxin for malignant glioma therapy: from bench to bedside. *J Neurooncol* 2003;65:37–48.
 30. Abdel-Fattah R, Xiao A, Bomgardner D, Pease CS, Lopes MB, Hussain IM. Differential expression of HOX genes in neoplastic and non-neoplastic human astrocytes. *J Pathol* 2006;209:15–24.
 31. Simeone A, Acampora D, D'Esposito M, Faiella A, Pannese M, Scotto L, Montanucci M, D'Alessandro G, Mavilio F, Boncinelli E. Posttranscriptional control of human homeobox gene expression in induced NTERA-2 embryonal carcinoma cells. *Mol Reprod Dev* 1989;1:107–15.
 32. Maroulakou IG, Spyropoulos DD. The study of HOX gene function in hematopoietic, breast and lung carcinogenesis. *Anticancer Res* 2003;23:2101–10.
 33. Guo M, Li J, Wan D, Gu J. KIAA0101 (OEACT-1), an expressionaly down-regulated and growth-inhibitory gene in human hepatocellular carcinoma. *BMC Cancer* 2006;6:109.
 34. Mizutani K, Onda M, Asaka S, Akaishi J, Miyamoto S, Yoshida A, Nagahama M, Ito K, Emi M. Overexpressed in anaplastic thyroid carcinoma-1 (OEATC-1) as a novel gene responsible for anaplastic thyroid carcinoma. *Cancer* 2005;103:1785–90.
 35. Hosokawa M, Takehara A, Matsuda K, Eguchi H, Ohigashi H, Ishikawa O, Shinomura Y, Imai K, Nakamura Y, Nakagawa H. Oncogenic role of KIAA0101 interacting with proliferating cell nuclear antigen in pancreatic cancer. *Cancer Res* 2007;67:2568–76.
 36. Scrideli CA, Carlotti CG Jr, Mata JF, Neder L, Machado HR, Oba-Shinjo SM, Rosenberg S, Marie SK, Tone LG. Prognostic significance of co-overexpression of the EGFR/IGFBP-2/HIF-2A genes in astrocytomas. *J Neurooncol* 2007;83:233–9.
 37. Verlinden L, Eelen G, Beullens I, Van Camp M, Van Hummelen P, Engelen K, Van Hellemont R, Marchal K, De Moor B, Foijer F, Te Rielle H, Beullens M, et al. Characterization of the condensin component Cnap1 and protein kinase Melk as novel E2F target genes downregulated by 1,25-dihydroxyvitamin D3. *J Biol Chem* 2005;280:37319–30.
 38. Seong HA, Gil M, Kim KT, Kim SJ, Ha H. Phosphorylation of a novel zinc-finger-like protein, ZPR9, by murine protein serine/threonine kinase 38 (MPK38). *Biochem J* 2002;361 (Part 3):597–604.
 39. Seong HA, Kim KT, Ha H. Enhancement of B-MYB transcriptional activity by ZPR9, a novel zinc finger protein. *J Biol Chem* 2003;278:9655–62.
 40. Lin ML, Park JH, Nishidate T, Nakamura Y, Katagiri T. Involvement of maternal embryonic leucine zipper kinase (MELK) in mammary carcinogenesis through interaction with Bcl-G, a pro-apoptotic member of the Bcl-2 family. *Breast Cancer Res* 2007;9:R17.
 41. Vulsteke V, Beullens M, Boudrez A, Keppens S, Van Eynde A, Rider MH, Stalmans W, Bollen M. Inhibition of spliceosome assembly by the cell cycle-regulated protein kinase MELK and involvement of splicing factor NIPPI1. *J Biol Chem* 2004;279:8642–7.
 42. Davezac N, Baldin V, Blot J, Ducommun B, Tassan JP. Human pEg3 kinase associates with and phosphorylates CDC25B phosphatase: a potential role for pEg3 in cell cycle regulation. *Oncogene* 2002;21:7630–41.
 43. Fournier MV, Martin KJ, Kenny PA, Xhaja K, Bosch I, Yaswen P, Bissell MJ. Gene expression signature in organized and growth-arrested mammary acini predicts good outcome in breast cancer. *Cancer Res* 2006;66:7095–102.
 44. Badouel C, Korner R, Frank-Vaillant M, Couturier A, Nigg EA, Tassan JP. M-phase MELK activity is regulated by MPF and MAPK. *Cell Cycle* 2006;5:883–9.
 45. Easterday MC, Dougherty JD, Jackson RL, Ou J, Nakano I, Paucar AA, Roobini B, Dianati M, Irvin DK, Weissman IL, Terskikh AV, Geschwind DH, et al. Neural progenitor genes. Germinal zone expression and analysis of genetic overlap in stem cell populations. *Dev Biol* 2003;264:309–22.
 46. Okamoto OK, Oba-Shinjo SM, Lopes L, Nagahashi Marie SK. Expression of HOXC9 and E2F2 are up-regulated in CD133+ cells isolated from human astrocytomas and associate with transformation of human astrocytes. *Biochim Biophys Acta* 2007;1769:437–42.
 47. Liu G, Yuan X, Zeng Z, Tunici P, Ng H, Abdulkadir IR, Lu L, Irvin D, Black KL, Yu JS. Analysis of gene expression and chemoresistance of CD133+ cancer stem cells in glioblastoma. *Mol Cancer* 2006;5:67.